Available online at www.sciencedirect.com
ScienceDirect
Tetrahedron
Tetrahedron 63 (2007) 1448–1458

A DFT study on the 1,3-dipolar cycloaddition reactions of *C*-(hetaryl) nitrones with methyl acrylate and vinyl acetate

Pedro Merino,[a,*] Tomas Tejero,[a] Ugo Chiacchio,[b] Giovanni Romeo[c] and Antonio Rescifina[b,*]

[a]*Departamento de Quimica Organica, Instituto de Ciencia de Materiales de Aragón, Universidad de Zaragoza, CSIC, Zaragoza E-50009, Spain*
[b]*Dipartimento di Scienze Chimiche, Università di Catania, Viale Andrea Doria 6, Catania 95125, Italy*
[c]*Dipartimento Farmaco-Chimico, Università di Messina, Viale SS. Annunziata, Messina 98168, Italy*

Received 19 October 2006; revised 18 November 2006; accepted 24 November 2006
Available online 13 December 2006

Abstract—The 1,3-dipolar cycloaddition of *C*-(hetaryl) nitrones with electron-poor and electron-rich alkenes is rationalized. The energetics of the cycloaddition reactions have been investigated through molecular orbital calculations at the B3LYP/6-31-G(d) theory level. By studying different reaction channels and reagent conformations the regio- and stereochemical preferences of the reaction are discussed.

1. Introduction

1,3-Dipolar cycloaddition reactions (DCR) between nitrones and alkenes provide polyfunctionalized isoxazolidines that are widely used in the synthesis of several nitrogen-containing products.[1] The availability of simple and efficient nitrones has been the driving force for the development of isoxazolidines as synthetic intermediates.[2] Given the importance of DCR, the mechanism of the reaction has been widely studied[3] and, during the last years, several computational studies have been reported to understand the origins of its regio- and stereoselectivities.[4] Nitrones bearing suitable substituents at the carbon atom are of particular interest since they can lead to substituted 1,3-aminoalcohols[5] or saturated nitrogen heterocycles such as pyrrolidines, pyrrolizidines and indolizidines[6] depending on the dipolarophile (Scheme 1). Within this context, glyoxylic acid-derived nitrones[7] **1** and *C*-(hetaryl) nitrones[8] **2** are valuable substrates because of the carboxylic acid unit present in the former and the masked functionalities available in the latter,[9] which allow a great number of further synthetic transformations. Particularly, the synthetic utility of *C*-(hetaryl) nitrones **2** has been demonstrated in our laboratories[8b,8c,10] and by other groups.[11]

The case of configurationally unstable nitrones **1** has been recently studied by us using DFT methods.[12] This approach showed to be quite convenient for obtaining reliable results at a low computational cost.[13] We have also reported experimental and semiempirical studies on the reaction between some hetaryl nitrones and electron-deficient alkenes.[14] However, the evaluation of a number of hetaryl nitrones **2**, bearing heterocyclic units of different electronic nature requires the use of the more valuable DFT methods. Therefore, this paper presents a complete DFT study of the cycloaddition reactions between hetaryl nitrones **2a–e** and both electron-poor and electron-rich dipolarophiles. For the purpose of comparison *C*-phenyl nitrone **2f** is also studied (Chart 1). The understanding of the transition structures involved will allow the prediction of selectivities of the reaction, expanding the synthetic applications of this method for preparing synthetic intermediates.

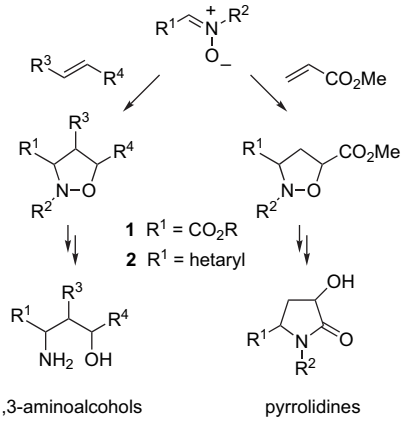

Scheme 1.

* Corresponding authors. Tel./fax: +34 976 762075 (P.M.); tel.: +39 095 738 5014; fax: +39 095 580 138 (A.R.); e-mail addresses: pmerino@unizar.es; arescifina@unict.it

0040–4020/$ - see front matter © 2006 Elsevier Ltd. All rights reserved.
doi:10.1016/j.tet.2006.11.073

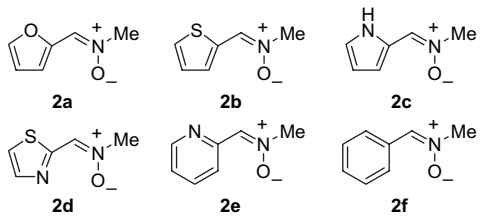

Chart 1.

2. Computational methods

Geometry optimizations of the critical points (reactants, transition structures and products) were carried out using DFT methods at the B3LYP/6-31G* level of theory.[15] Frequency calculation was used to confirm the nature of the stationary points. Transition structures were found to have only one negative eigenvalue with the corresponding eigenvector involving the formation of the newly created C–C and C–O bonds. Vibrational frequencies were calculated (1 atm, 298.15 K) for all B3LYP/6-31G* optimized structures and used, unscaled, to compute both ZPVE and activation energies. The electronic structures of critical points were studied by the natural bond orbital (NBO) method.[16] The enthalpy and entropy changes were calculated from standard statistical thermodynamic formulas.[17] The intrinsic reaction coordinates[18] (IRC analysis) were also calculated to analyze the mechanism in detail for all the transition structures obtained. DFT calculations were carried out with the G03 system of programs.[19]

We studied regio- and diastereoselectivities for the reaction of **2** with methyl acrylate **3** and vinyl acetate **4**. For each transition state the most stable conformations of methyl acrylate[20] and vinyl acetate[21] have been chosen. Both *E* and *Z* configurations of nitrones **2** have been evaluated. In addition, for nitrones **2a–e** *syn* and *anti* conformations[22] have also been calculated (obviously this does not apply for nitrone **2f**, for symmetry reasons since it has an only conformation for *E* and *Z* isomers). Once evaluated the stability of reactants the most stable conformations have been chosen for performing the study. Figure 1 displays the conformational features of the reaction partners. These conformations have been further employed for locating the corresponding transition states.

We have considered two reaction channels, *ortho* and *meta*, corresponding to the formation of 3,5- and 3,4-disubstituted

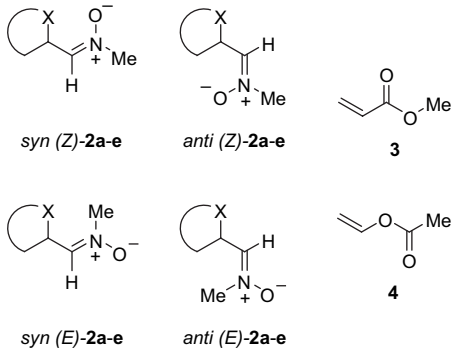

Figure 1. Reactants (for **2d** X refers to the sulfur atom).

isoxazolidines, respectively; *endo* and *exo* approaches to the most stable isomer of the corresponding nitrone completed the study. Consequently, four transition states leading to the four possible cycloadducts have been located for each nitrone and dipolarophile (a total of 48 transition structures have been located and fully optimized). The nomenclature used for defining stationary points is given in Scheme 2.

3. Results and discussion

3.1. Reactants

Relative energies shown in Table 1 indicate that energy differences among *E* and *Z* isomers of nitrones are quite significant, namely ca. 3–12 kcal/mol. In all cases the *Z*-isomer is the preferred one, consistent with previous findings reported for aldonitrones.[23] In the case of hetaryl nitrones **2a–e** relative energies among *syn* and *anti* conformations depend on the nature of the heterocyclic moiety. Thus, for *C*-(2-furyl) nitrone **2a** and *C*-(2-pyridyl) nitrone **2e** the *anti* conformation in which the heteroatom is orientated opposite to nitrone oxygen (*anti-Z* in Fig. 1) is the most stable. Differences of 5.0 and 7.4 kcal/mol are observed for **2a** and **2e**, respectively. The preference for such an *anti* conformation was also confirmed, in the case of nitrone **2e**, in solid state by means of an X-ray analysis.[24] On the other hand, nitrones **2b** and **2d** derived from 2-formylthiophene and 2-formylthiazole, respectively, showed a clear preference for *syn* conformers revealing the presence of a 1,5-interaction between the heterocyclic sulfur atom and the nitrone oxygen (Fig. 2). The optimized S–O distance was found to be 2.738 Å for **2b** and 2.721 Å for **2d**. These distances are substantially less than the sum of van der Waals radii (3.320 Å) and indicative of the expansion of the valence shell of the sulfur atom. Such an expansion can be characterized by the covalency ratio factor χ introduced by Weinhold and co-workers.[25] In the case of nitrones **2b** and **2d** χ is defined as follows:

$$\chi = \frac{(R_S + R_O) - d_{SO}}{(R_S + R_O) - (r_S + r_O)} \quad (1)$$

where R_S and R_O stand for van der Waals and r_S and r_O for covalent radii of sulfur and oxygen atom, d_{SO} being the optimized distance. For nitrones **2b** and **2d** the corresponding values of χ are 0.359 and 0.370, respectively, indicating a weak interaction but enough stabilization to induce the higher stability for *syn* conformation. The opposite charges on the sulfur atom (+0.330 for **2b** and +0.324 for **2d**) and on the oxygen atom (−0.489 for **2b** and −0.478 for **2d**) are mainly responsible for this electrostatic interaction. This sort of intramolecular donor–acceptor interactions are well-documented in literature[26] and are typical of 1,5-X,O systems (X=S, Se, Te). The preferred *syn* conformation for nitrone **2c** is clearly determined by the presence of an intramolecular hydrogen bond between the pyrrole NH group and the nitrone oxygen (d_{NH}=1.950 Å).

Also the Mulliken population analysis (MPA), which gives a qualitative indication for the amount of electron density shared by two atoms, confirms the above emerged picture; so we have found an O_4S_6 positive overlap density value

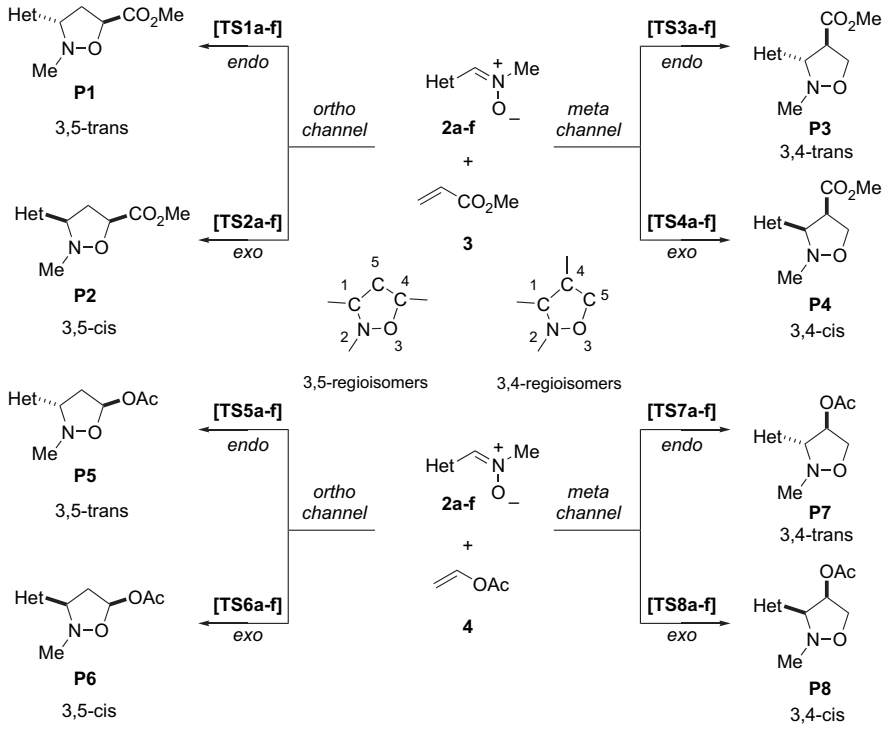

Scheme 2.

of 0.037 and 0.036 for the *syn-Z*-**2b** and *syn-Z*-**2d** nitrones, respectively, whose magnitude is in agreement with their higher stability. The analysis of the delocalization energies obtained with a Secondary-Order Perturbation Theory (SOPT) of the Fock matrix in NBO Basis points out that the secondary orbital interactions (SOI) outlined by the MPA are due to the principal stabilizing delocalization $nO_4 \rightarrow \sigma^*C_7–S_6$ (4.60 and 4.76 kcal/mol for *syn-Z*-**2b** and *syn-Z*-**2d**, respectively). For the *anti-Z*-**2b** the positive SOI interactions found for O_4H_{16} and O_4C_9 (0.021 and 0.006, respectively) are counterpoised by the N_3C_9 negative one (−0.014); the same trend is observed for the *anti-Z*-**2d** nitrone. In compound *syn-Z*-**2c** the hydrogen bond is evidenced by the O_4H_{16} positive SOI (0.060) due to a stabilizing $nO_4 \rightarrow \sigma^*N_6–H_{14}$ delocalization of 11.69 kcal/mol. On the contrary, in compound *anti-Z*-**2c** the two positive

Table 1. B3LYP/6-31G(d) free energies (*G*) (hartrees) relative free energies (Δ*G*) (kcal/mol), electronic energies (*E*) (hartrees) and relative electronic energies (Δ*E*) (kcal/mol)

	E	Δ*E*[a]	*G*	Δ*G*[a]	Dipole moment
anti (*Z*)-**2a**	−437.824195	0.00	−437.864981	0.00	2.52
syn (*Z*)-**2a**	−437.816165	5.04	−437.857399	4.76	3.51
anti (*E*)-**2a**	−437.814080	6.35	−437.855394	6.02	4.21
syn (*E*)-**2a**	−437.815563	5.42	−437.857441	4.73	4.04
anti (*Z*)-**2b**	−760.804848	2.02	−760.847035	1.81	2.52
syn (*Z*)-**2b**	−760.808070	0.00	−760.849913	0.00	3.55
anti (*E*)-**2b**	−760.794507	8.51	−760.836948	8.14	4.04
syn (*E*)-**2b**	−760.794872	8.28	−760.838253	7.32	3.66
anti (*Z*)-**2c**	−417.953993	7.37	−417.995303	6.90	4.87
syn (*Z*)-**2c**	−417.965743	0.00	−418.006306	0.00	2.29
anti (*E*)-**2c**	−417.946464	12.10	−417.988081	11.44	3.71
syn (*E*)-**2c**	−417.943959	13.67	−417.985552	13.02	4.35
anti (*Z*)-**2d**	−776.852976	8.75	−776.895490	8.12	3.74
syn (*Z*)-**2d**	−776.866923	0.00	−776.908430	0.00	2.11
anti (*E*)-**2d**	−776.857703	5.79	−776.900030	5.27	3.52
syn (*E*)-**2d**	−776.852288	9.18	−776.894761	8.58	4.24
anti (*Z*)-**2e**	−456.066205	0.00	−456.108556	0.00	1.22
syn (*Z*)-**2e**	−456.054185	7.54	−456.097330	7.04	4.36
anti (*E*)-**2e**	−456.060146	3.80	−456.102894	3.55	4.17
syn (*E*)-**2e**	−456.052986	8.30	−456.095573	8.15	5.10
(*Z*)-**2f**	−440.014717	0.00	−440.057304	0.00	3.13
(*E*)-**2f**	−440.004172	6.62	−440.046849	6.56	3.87
3	−306.365295	—	−306.402235	—	1.50
4	−306.369179	—	−306.407043	—	1.73

[a] Referred for each series.

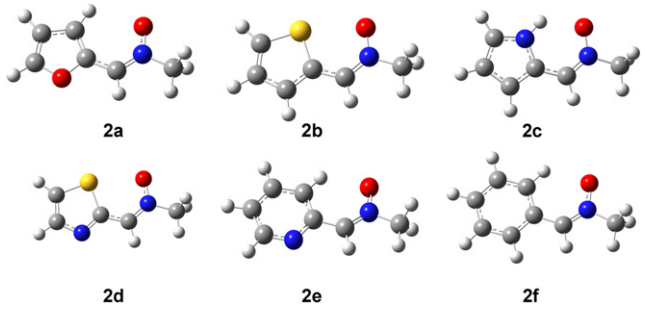

Figure 2. B3LYP/6-31G(d) optimized structures of the reactants.

SOI interactions found for O_4H_{17} and O_4C_9 (0.018 and 0.006, respectively) are counterpoised by the N_3C_9 and N_3H_{17} negative ones (−0.011 and −0.005, respectively).

In general, the dipole moments are lower in *Z*-isomers for a given conformation. Thus, the lowest values correspond to the most stable conformations, the only exception being *C*-(2-thienyl) nitrone **2b**. The dipole moment for *syn*-*Z*-**2b** (3.55) is greater than that of its respective *anti*-*Z* isomer (Table 1). Indeed, the largest dipole moment corresponds to *syn*-*Z*-**2b** in which the sulfur atom and the nitrone oxygen are orientated in a parallel way as a consequence of the above mentioned 1,5-S,O stabilizing interactions, and it is in accord to the concordance vectors of the independent dipole moments for thiophene and nitrone moieties. In all the other more stable nitrones the same vectors are discordant.

3.2. DFT analysis based on the reactivity indices

These 1,3-DC reactions have been analyzed using the global indexes, as defined in the context of DFT,[27] which are useful tools to understand the reactivity of molecules in their ground states. The electronic chemical potential μ, that is the negative of electronegativity χ, is usually associated with the charge transfer ability of the system in its ground state geometry and it can be approximated, using Koopmans' theorem, to the half value of the sum of the one-electron energies of the FMOs HOMO and LUMO.[28] The chemical hardness η is considered to be a measure of the stability of a system: the system having the maximum hardness being the most stable.[29] Essentially the hardness is approximated to be the difference between LUMO and HOMO energies. The chemical softness parameter S is strictly related to the chemical hardness and it is due to the inverse of 2η.[28]

Besides these indexes it is also possible to define the global electrophilicity power ω, which measures the stabilization in energy when the system acquires an additional electronic charge ΔN from the environment. The approximate expression for ω, in the ground state parabola model, is[30]

$$\omega = \frac{\mu^2}{2\eta} \tag{2}$$

and it is a useful descriptor of reactivity that allows a quantitative classification of the global electrophilic character of a molecule within a relative scale. Both Diels–Alder reactions[31] and DCR[32] can be evaluated using such an absolute scale. Moreover, the maximum amount of electronic charge that the electrophile system may accept is given by:

$$\Delta N_{\max} = -\frac{\mu}{\eta} \tag{3}$$

The values of μ, η, S and ω for compounds *anti*-*Z*-**2a**,**e**, *syn*-*Z*-**2b**–**d**, *Z*-**2f**, **3** and **4**, calculated with the reported formulas, are listed in Table 2. The electronic chemical potential, μ, of all nitrones **2** is less than that of the dipolarophile **3**, thereby indicating that a net charge transfer will take place from the dipole to the dipolarophile, i.e. $HOMO_{dipole}-LUMO_{dipolarophile}$ interaction, in agreement with the charge transfer analysis performed at the corresponding TSs (vide infra). The same trend, but with a minor difference between the μ values, is observed for dipoles **2a**, **2b**, **2c** and **2f** in comparison with **4**, indicating only a slight charge transfer between the two reactants. This expectation is in contrast with the charge transfer analysis performed at the corresponding TSs respect to the electron flow but is in agreement with respect to the magnitude. Vice versa, the chemical potential of **2d** and **2e** is higher than that of **4**, thereby indicating that a net charge transfer will take place from dipolarophile to dipole.

Indeed, the electrophilicity differences, $\Delta\omega$, between **2** and **3**,**4** ($\Delta\omega$=0.10−0.79 eV) indicate a lower polar character for these cycloadditions and their values are characteristic of non-polar (pericyclic) reactions[31,32] as is also indicated by the low charge transfer found in all cases. Moreover, the dipolarophile **3** presents a high electrophilicity value and, according to the absolute scale of electrophilicity based on the ω index,[30] it can be classified as strong electrophile; on the contrary, the dipolarophile **4** has a larger electrophilicity value (0.96 eV) than that expected due to the presence of the carboxylate group (note that the electrophilicity of methyl vinyl ether, which is classified as a good nucleophile, is 0.42 eV). Thus, using the same consideration as for **3**, compound **4** can only be considered moderate electrophilic. The same analysis, extended to dipoles **2** tell us that nitrones **2d** and **2e** are strong electrophiles whereas the remaining

Table 2. HOMO, LUMO and global properties (HOMO, LUMO, electronic chemical potential μ, chemical hardness η and chemical softness S values are in au; electrophilicity power ω values are in eV)

	HOMO	LUMO	μ	η	S	ω	$\Delta N_{\max}$
anti (*Z*)-**2a**	0.19241	0.04271	−0.11756	0.14970	3.340	1.26	0.79
syn (*Z*)-**2b**	0.19514	0.04870	−0.12192	0.14644	3.414	1.38	0.83
syn (*Z*)-**2c**	0.18345	0.03320	−0.10833	0.15025	3.328	1.06	0.72
syn (*Z*)-**2d**	0.21260	0.06397	−0.13829	0.14863	3.364	1.75	0.93
anti (*Z*)-**2e**	0.21244	0.05654	−0.13449	0.15590	3.207	1.58	0.86
(*Z*)-**2f**	0.20230	0.04650	−0.12440	0.15580	3.209	1.35	0.80
3	−0.27279	−0.04404	−0.15842	0.22875	2.186	1.49	0.69
4	0.24948	0.01036	−0.12992	0.23912	2.091	0.96	0.54

Table 3. B3LYP/6-31G(d) relative free energies (ΔG) (kcal/mol) and relative electronic energies (ΔE) (kcal/mol) for the reaction of nitrones **2a–f** with methyl acrylate **3**

Nitrone	TS	Direct ΔE[a]	Inverse ΔE[b]	Direct ΔG[a]	Inverse ΔG[b]	Product	Direct ΔE[a]	Direct ΔG[a]
2a	**TS1a**	16.91	26.57	29.73	26.44	**P1a**	−9.66	3.29
	TS2a	19.22	30.95	31.89	30.99	**P2a**	−11.73	0.89
	TS3a	16.13	25.27	29.15	25.60	**P3a**	−9.14	3.55
	TS4a	18.33	26.14	31.34	26.23	**P4a**	−7.80	5.10
2b	**TS1b**	17.90	27.24	30.89	27.23	**P1b**	−12.50	0.00
	TS2b	21.10	31.27	33.98	31.77	**P2b**	−13.33	−1.46
	TS3b	16.78	25.21	29.86	25.75	**P3b**	−11.59	0.45
	TS4b	19.30	26.87	32.43	26.48	**P4b**	−10.72	2.28
2c	**TS1c**	18.49	25.53	31.47	25.87	**P1c**	−7.04	5.60
	TS2c	19.29	24.42	32.45	24.58	**P2c**	−5.14	7.88
	TS3c	17.27	23.73	30.35	24.09	**P3c**	−6.45	6.26
	TS4c	19.30	25.44	32.46	25.07	**P4c**	−6.13	7.39
2d	**TS1d**	17.41	29.05	30.31	28.94	**P1d**	−11.64	1.37
	TS2d	20.27	28.88	33.06	29.04	**P2d**	−8.61	4.02
	TS3d	17.29	28.39	30.39	28.78	**P3d**	−11.10	1.61
	TS4d	19.53	28.31	32.66	28.08	**P4d**	−8.78	4.58
2e	**TS1e**	15.31	29.25	28.21	29.23	**P1e**	−13.94	−1.02
	TS2e	17.34	31.26	30.22	31.18	**P2e**	−13.92	−0.96
	TS3e	15.39	28.78	28.38	28.90	**P3e**	−13.39	−0.52
	TS4e	17.62	29.30	30.63	29.02	**P4e**	−11.68	1.60
2f	**TS1f**	15.85	28.51	28.71	28.54	**P1f**	−12.67	0.18
	TS2f	18.38	32.64	31.41	32.79	**P2f**	−14.26	−1.38
	TS3f	15.00	27.27	28.03	27.50	**P3f**	−12.27	0.52
	TS4f	17.62	28.45	31.02	28.27	**P4f**	−10.83	2.75

[a] Referred to nitrone **2**+**3** (see Table 1 for values).
[b] Referred to the corresponding products.

ones are moderate electrophiles. Being the ω index of **4** less than those of all nitrones, it will act as nucleophile with a net charge transfer to compounds **2**, in total accord, this time, to the analysis performed at the corresponding TSs (see below). This is because the electrophilicity index encompasses both the propensity of the electrophile to acquire an additional electronic charge driven by μ^2, and the resistance of the system to exchange electronic charge with the environment described by η, simultaneously.

Considering the difference in electrophilicity indexes, the more favourable interactions will take place between **2c**, the less electrophilic species, and **3**, for the acrylate DCR and between **2d** and **4** for the acetate one. From the hardness values,[33] reported in Table 2, it emerges that **2b** is slightly more aromatic than **2a**, in agreement with experimental data.

3.3. Cycloadditions with methyl acrylate

3.3.1. Energies of the transition structures. The absolute and relative free and electronic energies with respect to reactants for the 24 transition structures located for the reaction between nitrones **2** and methyl acrylate **3** are collected in Table 3. The energy differences between products and reactants are given, too. The analysis of relative electronic (ΔE) and free energies (ΔG) shows that, in general, *endo* attacks (leading to trans adducts) are preferred to the corresponding *exo* approaches (leading to cis adducts). There is not a clear preference between *ortho* and *meta* channels, thus predicting that mixtures of 3,5 and 3,4 adducts will be obtained. This situation is particularly manifested for nitrones **2a**, **2d**, **2e** and **2f** for which differences of less than 1.0 kcal/mol is observed between *endo*/*ortho* and *endo*/*meta* pathways, corresponding to **TS1a–f** and **TS3a–f**, respectively. Nitrones **2b** and **2c** presented differences between those transition structures of 2.39 and 1.22 kcal/mol, respectively. The same conclusion can be drawn from the analysis of the relative free energies (ΔG), no noticeable differences being observed for ΔG values when compared with ΔE values. The lower calculated activation energies for the reactions of nitrones **2** with methyl acrylate correspond to *C*-phenyl (**2f**) and *C*-(2-pyridyl) (**2e**) nitrones. On the other hand, the highest energy barrier was observed for *C*-(2-thiazolyl) nitrone **2d**. Nevertheless, the observed maximum differences for the more stable transition structure corresponding to all studied nitrones were 2.29 kcal/mol and 2.32 kcal/mol for ΔE and ΔG, respectively. These differences are rather small considering the different electronic nature of the nitrones **2a–f**, thus indicating the same general behaviour for these cycloadditions.

On the basis of the reverse barrier energies given in Table 2 it is possible to assume the reversibility of the reaction, particularly when it is carried out in toluene or chloroform at reflux. Under these conditions a certain thermodynamic control should be observed, the corresponding more stable product being obtained predominantly. However, this prediction is only slightly confirmed from the experimental results. For nitrone **2a**, compound **P1a** was obtained predominantly for whatever the conditions used were. In all cases mixtures of compounds **P1a**, **P2a** and **P3a** were obtained. Only when the reaction was carried out under kinetic control (neat, −18 °C) compound **P1a** was obtained as the only product of the reaction.[14] This result can be considered to be in agreement with the calculations since the observed differences between **TS1a** and **TS3a** ($\Delta\Delta E$=0.78 kcal/mol; $\Delta\Delta G$=0.58 kcal/mol) are within the experimental error. A

similar concordance is found in the case of *C*-(2-pyridyl) nitrone **2e** for which energy differences between both transition states and final products are lower than 1 kcal/mol. On the other hand, experimental results are not so well predicted for the case of *C*-(2-thienyl) nitrone **2b**. Whereas the experimental results are quite similar to those observed for **2a** and **2e**, calculations predict the preferential achievement of adducts **P3b** and **P2b** under kinetic and thermodynamic control, respectively.

For **TS1a–f** and **TS3a–f**, which correspond to the transition structures for the *endo* approach in the *ortho* and *meta* channels, respectively, MPA provides some evidence for secondary orbital interaction (SOI) between the two reactants.[34] In fact the **TS1a** shows a positive overlap density of 0.016, 0.006 and 0.002 for O_3H_{17}, C_4O_7 and $H_{16}O_{28}$, respectively, due to stabilizing $nO_3 \rightarrow \sigma^*C_9–H_{17}$ (1.80 kcal/mol), $\pi O_3–C_4 \rightarrow \sigma^*C_9–H_{17}$ (0.60 kcal/mol), $nO_7 \rightarrow \pi^*O_3–C_4$ (1.02 kcal/mol) and $\sigma C_6–H_{16} \rightarrow \pi^*C_{21}–C_{26}$ (0.28 kcal/mol) delocalization energies; while in **TS3a** only the O_4H_{17} (0.020) positive overlap was observed. On the contrary, these interactions do not appear for the *exo* approach, whereas for **TS2b–d** and **TS4b–d**, emerged a slightly positive overlap between the sulfur or nitrogen atom of hetaryl moiety and the carboxylic oxygen of acrylate (0.005–0.010). This is completely in accord to the major stability of **TSs1** and **TSs3** versus **TSs2** and **TSs4** due to the strongest SOI achieved in the *endo* approach.

Moreover, in **TS2c** the hydrogen bond present in the nitrone reagent is shifted to the carboxylic oxygen of acrylate as evidenced by the high value of O_3H_{29} positive overlap (0.056) due to a stabilizing $nO_3 \rightarrow \sigma^*N_{28}–H_{29}$ delocalization energy of 10.83 kcal/mol.

3.3.2. Geometries of the transition structures. The optimized geometries of 12 transition structures corresponding to the reaction of hetaryl nitrones **2a–f**, leading to the corresponding adducts **P1–P4** are illustrated in Figures 3 and 4. Only the more stable and competitive 3,5-*trans* and 3,4-*trans* (*endo* approaches) transition structures are shown (the rest of geometries are available from the authors). The corresponding selected geometric parameters are given in Table 4.

As expected for 1,3-dipolar cycloadditions all transition structures are asynchronous. *meta* Transition structures are more asynchronous than the corresponding *ortho* counterparts for the *endo* approaches (Fig. 3 and Table 4), and in spite of the significant asynchronicity the values are within the range of a concerted process. Similar differences are observed for all studied *C*-(hetaryl) nitrones **2**. Forming $C_1–C_5$ bond lengths (2.013–2.045 Å) are shorter than $O_3–C_4$ distances (2.202–2.240 Å) for the *ortho* transition structures. On the other hand, the opposite is found for *meta* transition structures, with forming $O_3–C_5$ bond lengths (1.825–1.873 Å) being shorter than $C_1–C_4$ distances (2.318–2.337 Å). Such a reversed situation is in agreement with previously studied 1,3-dipolar cycloadditions with

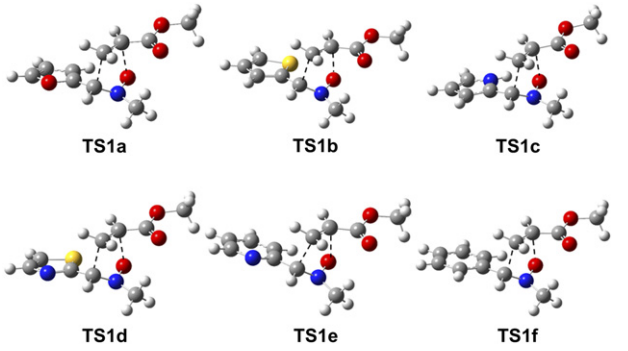

Figure 3. Optimized geometries at B3LYP/6-31G(d) level for *ortho* (3,5-*endo*) transition structures leading to **P1a–f**.

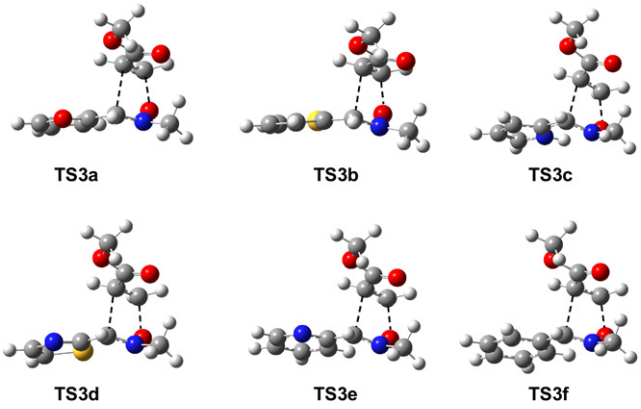

Figure 4. Optimized geometries at B3LYP/6-31G(d) level for *meta* (3,4-*endo*) transition structures leading to **P3a–f**.

Table 4. Selected geometric parameters for transition structures illustrated in Figures 3 and 4

TS	$C_1–C_5$,[a] $C_1–C_4$[b]	$O_3–C_4$,[a] $O_3–C_5$[b]	$O_3–N_2–C_1–C_5$,[a] $O_3–N_2–C_1–C_4$[b]	$O_3–C_4–C_5–C_1$,[a] $O_3–C_5–C_4–C_1$[b]
TS1a	2.030	2.212	−59.05	−11.91
TS3a	2.337	1.836	−51.06	−1.18
TS1b	2.308	2.208	−58.39	−11.60
TS3b	2.330	1.835	−51.02	0.22
TS1c	2.013	2.202	−58.87	−12.77
TS3c	2.329	1.825	−50.68	−0.27
TS1d	2.020	2.231	−58.95	−10.62
TS3d	2.300	1.867	−50.96	0.33
TS1e	2.034	2.240	−57.71	−11.12
TS3e	2.318	1.873	−49.70	−0.06
TS1f	2.045	2.215	−57.30	−10.78
TS3f	2.335	1.856	−48.86	−0.20

[a] Referred to *ortho* transition structures **TS1a–f**.
[b] Referred to *meta* transition structures **TS3a–f**.

electron-deficient dipolarophiles.[12] Moreover, taking into consideration that C–O sigma bonds are shorter than C–C sigma bonds, the *meta* channel can be envisioned in some extent to be near to a Michael addition in which the nitrone oxygen acts as a nucleophile. On the contrary, the *ortho* channel, representing a typical asynchronous process can be considered as an early transition state as indicates the relative long distance of the forming O_3–C_4 bonds. This change of synchronicity for the *ortho* and *meta* channels is controlled by a large bond formation at the β conjugate position of **3**.[35]

The conformation of the forming isoxazolidine rings, defined by O_3–N_2–C_1–C_4–C_5 and O_3–N_2–C_1–C_5–C_4 atoms for *meta* and *ortho* channels, respectively, is similar for both channels, and no significant differences are observed between the studied nitrones. All transition structures corresponding to *endo* approaches (Table 4) show negative values, in the range of −48.86° to −59.05°, of ⟨O_3–N_2–C_1–C_4(C_5) dihedral angle, the more negative values corresponding to the *ortho* channel. Smaller values (0.33° to −12.77°) were found for the ⟨O_3–C_5(C_4)–C_4(C_5)–C_1 dihedral angle, and in this case, clear differences are observed between the two studied channels. Transition structures corresponding to the *meta* channel (3,4-*endo* attack) present values near to 0°, indicating that four atoms are in a plane, the only out-of-plane atom being the nitrogen one. On the other hand, transition structures corresponding to the *ortho* channel (3,5-*endo* attack) present higher absolute values, in the range of −10.62° to −12.77°.

3.3.3. Bond order and charge analysis. The concept of bond order (BO) can be utilized to obtain a more deeper analysis of the extent of bond formation or bond breaking along a reaction pathway. This theoretical tool has been used to study the molecular mechanism of chemical reactions. To follow the nature of the formation process for C_1–C_5 (C_1–C_4) and C_4–O_3 (C_5–O_3) bonds, the Wiberg bond indexes[36] have been computed by using the NBO 5.0 population analysis package. The results are included in Table 5.

The general analysis of the bond order values for all the TSs structures showed that the cycloaddition process is asynchronous with an interval of 0.285–0.484 and 0.275–0.520 for the *ortho* and *meta* channels, respectively. Moreover, for the *ortho* channel the BOs for the forming C_1–C_5 bonds are in the range of 0.449–0.484 and have greater values than that for the forming C_4–O_3 bonds that are in the range of 0.285–0.315. Instead, for the *meta* channel the BOs for the forming C_1–C_4 bonds (0.275–0.322) have lesser values than that for the forming C_5–O_3 (0.468–0.520). These data show a change of asynchronicity on the bond formation process for the two regioisomeric pathways with an extent of asynchronicity more marked for the channel.

The natural population analysis[37] allows to evaluate the charge transferred between the two reactants at the TSs geometry. The charge transfer in terms of the residual charge on the nitrone, for all the optimized TSs, is shown in Table 5. Although the positive values are indicative of an electron flow from the HOMO of nitrone to the LUMO of the methyl acrylate, in accord to the chemical potential analysis, their magnitudes revealed an almost neutral reaction.

Table 5. Bond orders (Wiberg indexes) for the two forming bonds in the TSs and charge transfer (au) in terms of the residual charge of the nitrone fragment in the transition state

Nitrone	TS	C_1–C_5,[a] C_1–C_4[b]	C_4–O_3,[a] C_5–O_3[b]	NPA q_{CT} (e)
2a	**TS1a**	0.469	0.302	0.07
	TS2a	0.456	0.315	0.05
	TS3a	0.305	0.514	0.08
	TS4a	0.292	0.500	0.08
2b	**TS1b**	0.472	0.301	0.06
	TS2b	0.458	0.314	0.05
	TS3b	0.309	0.514	0.08
	TS4b	0.301	0.492	0.07
2c	**TS1c**	0.484	0.304	0.06
	TS2c	0.471	0.305	0.08
	TS3c	0.309	0.520	0.09
	TS4c	0.275	0.509	0.11
2d	**TS1d**	0.473	0.295	0.05
	TS2d	0.456	0.305	0.03
	TS3d	0.322	0.493	0.05
	TS4d	0.319	0.472	0.04
2e	**TS1e**	0.462	0.285	0.06
	TS2e	0.449	0.296	0.05
	TS3e	0.312	0.485	0.06
	TS4e	0.306	0.468	0.06
2f	**TS1f**	0.462	0.292	0.07
	TS2f	0.450	0.304	0.05
	TS3f	0.304	0.496	0.08
	TS4f	0.299	0.476	0.07

[a] Referred to 3,5-regioisomers.
[b] Referred to 3,4-regioisomers.

3.4. Cycloadditions with vinyl acetate

3.4.1. Energies of the transition structures. The absolute and relative free and electronic energies with respect to reactants for the 24 transition structures located for the reaction between nitrones **2** and vinyl acetate **4** are collected in Table 6. The energy differences between products and reactants are given, too.

The calculated activation energies for the reaction of nitrones with vinyl acetate **4** favour the *ortho* channel (leading to 3,5 adducts) over the *meta* one (leading to 3,4 adducts), predicting the formation of mixtures due to the small differences between energy barriers (18.63–23.99 kcal/mol), which fall within the experimental error values. Inclusion of the activation entropy raises the activation free energies in the range of 31.19–37.22 kcal/mol showing the same trend, i.e. preferential formation of 3,5-regioisomers. As expected for electron-rich dipolarophiles the *exo* adducts leading to cis compounds are predicted to be formed preferentially, although the small differences between *endo* and *exo* transition structures ($\Delta\Delta E$=0.54–1.14 kcal/mol and $\Delta\Delta G$=0.46–1.45 kcal/mol) actually predict the obtainment of mixtures of cis and trans products. This prediction agrees well with the experimentally observed cis/trans ratio for the cycloaddition of vinyl acetate with *C*-(2-furyl) nitrones (60:40–100:0), *C*-phenyl nitrones (38:62) and *C*-(2-pyridyl) nitrones (40:60–30:70).[38]

As in the case of methyl acrylate the lower calculated activation energies correspond to *C*-phenyl and *C*-(2-pyridyl) nitrones **2f** and **2e**, respectively. The higher calculated values correspond to the *C*-(2-thienyl) and *C*-(2-pyrrolyl) nitrones

Table 6. B3LYP/6-31G(d) relative free energies (ΔG) (kcal/mol) and relative electronic energies (ΔE) (kcal/mol) for the reaction of nitrones **2a–f** with vinyl acetate **4**

Nitrone	TS	Direct ΔE[a]	Inverse ΔE[b]	Direct ΔG[a]	Inverse ΔG[b]	Product	Direct ΔE[a]	Direct ΔG[a]
2a	**TS5a**	21.33	40.71	34.30	40.90	**P5a**	−19.39	−6.60
	TS6a	20.32	39.45	33.14	39.35	**P6a**	−19.14	−6.21
	TS7a	22.74	36.36	35.56	36.20	**P7a**	−13.62	−0.64
	TS8a	23.60	36.91	36.83	36.46	**P8a**	−13.31	0.37
2b	**TS5b**	22.03	40.99	35.05	40.97	**P5b**	−20.98	−7.72
	TS6b	21.49	40.78	34.59	40.82	**P6b**	−21.32	−8.03
	TS7b	22.77	35.25	36.07	35.18	**P7b**	−14.51	−0.92
	TS8b	23.46	36.11	37.33	36.30	**P8b**	−14.67	−0.77
2c	**TS5c**	22.13	37.43	35.17	37.74	**P5c**	−15.31	−2.56
	TS6c	21.48	37.49	33.89	37.04	**P6c**	−16.01	−3.15
	TS7c	23.78	33.39	36.99	33.58	**P7c**	−9.61	3.41
	TS8c	23.87	31.76	37.58	31.40	**P8c**	−7.89	6.18
2d	**TS5d**	21.56	40.56	34.50	40.52	**P5d**	−19.00	−6.02
	TS6d	20.73	39.23	33.80	39.50	**P6d**	−18.50	−5.70
	TS7d	23.79	36.67	36.71	36.55	**P7d**	−12.88	0.16
	TS8d	23.99	36.15	37.22	35.98	**P8d**	−12.16	1.25
2e	**TS5e**	19.77	41.37	32.64	41.37	**P5e**	−21.60	−8.73
	TS6e	18.63	39.77	31.19	39.34	**P6e**	−21.13	−8.16
	TS7e	22.24	37.47	34.83	36.97	**P7e**	−15.22	−2.14
	TS8e	23.13	37.83	36.20	37.83	**P8e**	−14.70	−1.63
2f	**TS5f**	20.32	41.97	33.32	42.01	**P5f**	−21.65	−8.68
	TS6f	19.32	41.02	31.91	40.42	**P6f**	−21.70	−8.52
	TS7f	20.67	36.82	33.95	36.78	**P7f**	−16.15	−2.83
	TS8f	22.40	38.22	36.12	38.00	**P8f**	−15.82	−1.88

[a] Referred to nitrone **2+4** (see Table 1 for values).
[b] Referred to the corresponding products.

2b and **2c**, respectively, with a minimum difference of 0.01 kcal/mol in the activation energy. When considering the free activation energies, the highest value corresponds to nitrone **2b**. It is possible to assume some reversibility of the process by considering the reverse free energy barriers. However, since the higher stability of the final products corresponds to 3,5-regioisomers both kinetic and thermodynamic pathways lead to the same adducts. Indeed, as mentioned above, no 3,4-regiosiomers are experimentally observed for this reaction.

Also in this case, MPA provides some evidence for the major stability of **TS6a–f**, corresponding to the transition structures for the *exo* approach in the *ortho* channel, over the corresponding **TS5a–f**, due to SOI effect. In fact, the **TS6a** shows a positive overlap density of 0.004 for O_7C_{26} and $O_{15}C_{16}$, which implies an interaction with the aromatic ring, another positive interaction for O_4C_8 and a negative ones, of −0.017, for O_4H_9; on the contrary, **TS5a** shows a positive overlap density of 0.004 for O_4C_6 and a negative ones of −0.020 for O_4H_9 therefore accounting for its minor stability. Similar interactions are involved in **TS6a** (O_4C_6=0.005 and O_4O_9=−0.017), and **TS6b** (O_4C_6=0.004 and O_4O_9=−0.021). These interactions are reversed for **TS7a**,**b** and **TS8a**,**b** justifying their preference for the *endo* approach.

3.4.2. Geometries of the transition structures. The optimized geometries of 12 transition structures corresponding to the reaction of hetaryl nitrones **2a–f**, leading to the corresponding adducts **P5–P8** are illustrated in Figures 5 and 6. Only the more stable and competitive 3,5-*trans* (*endo* approaches) and 3,5-*cis* (*exo* approaches) transition structures are shown (the rest of geometries are available

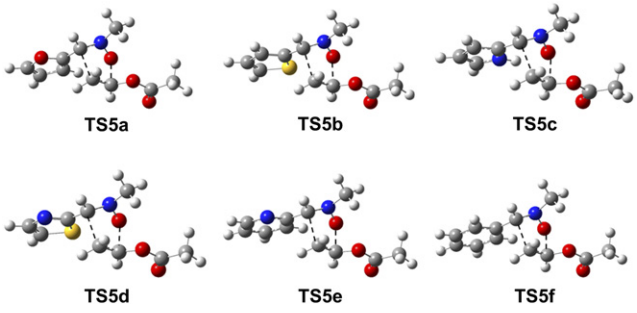

Figure 5. Optimized geometries at B3LYP/6-31G(d) level for *ortho* (3,5-*endo*) transition structures leading to **P5a–f**.

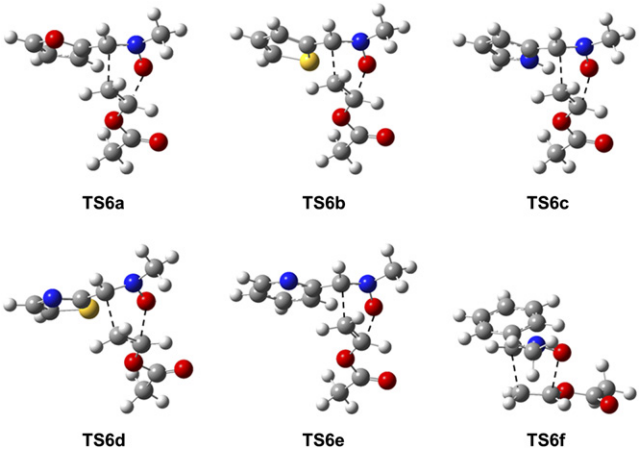

Figure 6. Optimized geometries at B3LYP/6-31G(d) level for *ortho* (3,5-*exo*) transition structures leading to **P6a–f**.

Table 7. Selected geometric parameters for transition structures illustrated in Figures 5 and 6

TS	C_1–C_5[a]	O_3–C_4[b]	O_3–N_2–C_1–C_5	O_3–C_4–C_5–C_1
TS5a	2.168	2.096	55.26	2.60
TS6a	2.153	2.131	55.90	10.07
TS5b	2.159	2.100	55.35	1.83
TS6b	2.159	2.127	55.26	0.50
TS5c	2.182	2.075	54.92	2.70
TS6c	2.164	2.111	55.73	10.25
TS5d	2.143	2.127	55.38	1.24
TS6d	2.132	2.165	56.21	7.51
TS5e	2.165	2.125	53.52	0.77
TS6e	2.149	2.161	54.59	10.83
TS5f	2.178	2.102	53.33	0.72
TS6f	2.164	2.134	54.46	10.30

[a] Referred to 3,5-regioisomers.
[b] Referred to 3,4-regioisomers.

from the authors). The corresponding selected geometric parameters are given in Table 7.

The corresponding lengths of the forming bonds are closer for the reactions with vinyl acetate than for the reactions with methyl acrylate thus indicating a lower asynchronicity of the cycloaddition process. The length of the C_1–C_5 and O_3–C_4 forming bonds are in the range of 2.132 to 2.164 Å and 2.111 to 2.165 Å, respectively for the favoured *exo* approach. These values, when compared with those corresponding to the *endo* approach (Table 7) indicate a minor extent of the asynchronicity for the *exo* approach. By considering that C–O sigma bonds are shorter than C–C sigma bonds, the close values found for the forming bond lengths clearly show a concerted process.

A similar trend to that found for methyl acrylate is observed for the geometrical disposition of the forming isoxazolidines. Quite similar values are observed for $\langle O_3$–N_2–C_1–C_5 (53.33°–56.21°) dihedral angle although with an opposite sign. Close values to 0°, indicating coplanarity of O_3, C_1, C_4 and C_5 atoms, are found for $\langle O_3$–C_4–C_5–C_1 dihedral angle in the case of 3,5-*endo* transition structures. Small positive values (7.51°–10.83°) are observed for the same dihedral angle in the case of 3,5-*exo* transition structures.

3.4.3. Bond order and charge analysis. The general analysis of the bond order values for all the TSs structures corresponding to the cycloaddition reactions with vinyl acetate showed that the cycloaddition process is slightly asynchronous with an interval, in the Wiberg bond indexes, of 0.310–0.410 and 0.373–0.417 for the *ortho* and *meta* channels, respectively (Table 8). Moreover, for the *ortho* channel the BOs for the forming C_1–C_5 bonds are in the range of 0.393–0.410 and have greater values than that for the forming C_4–O_3 bonds that are in the range of 0.310–0.349. Instead, for the *meta* channel the BOs for the forming C_1–C_4 bonds (0.373–0.405) have lesser values than that for the former C_5–O_3 (0.384–0.417). These data show a change of asynchronicity on the bond formation process for the two regioisomeric pathways with the *ortho* channel slightly more asynchronous of the *meta* one.

The charge transfer, evaluated by the natural population analysis, in terms of the residual charge on the nitrone, for all the optimized TSs, is shown in Table 8. The negative

Table 8. Bond orders (Wiberg indexes) for the two forming bonds in the TSs and charge transfer (au) in terms of the residual charge of the nitrone fragment in the transition state

Nitrone	TS	C_1–C_5,[a] C_1–C_4[b]	C_4–O_3,[a] C_5–O_3[b]	NPA q_{CT} (e)
2a	**TS5a**	0.398	0.349	−0.03
	TS6a	0.396	0.328	−0.04
	TS7a	0.392	0.397	−0.01
	TS8a	0.379	0.415	−0.02
2b	**TS5b**	0.404	0.345	−0.03
	TS6b	0.403	0.324	−0.04
	TS7b	0.395	0.396	−0.01
	TS8b	0.378	0.417	−0.02
2c	**TS5c**	0.410	0.345	−0.03
	TS6c	0.408	0.327	−0.03
	TS7c	0.405	0.395	−0.01
	TS8c	0.385	0.414	−0.01
2d	**TS5d**	0.408	0.336	−0.05
	TS6d	0.405	0.315	−0.06
	TS7d	0.399	0.391	−0.04
	TS8d	0.386	0.409	−0.05
2e	**TS5e**	0.395	0.331	−0.04
	TS6e	0.394	0.310	−0.05
	TS7e	0.391	0.384	−0.03
	TS8e	0.375	0.402	−0.03
2f	**TS5f**	0.394	0.340	−0.03
	TS6f	0.393	0.320	−0.04
	TS7f	0.387	0.388	−0.01
	TS8f	0.373	0.410	−0.02

[a] Referred to 3,5-regioisomers.
[b] Referred to 3,4-regioisomers.

values are indicative of an electron flow from the HOMO of the vinyl acetate to the LUMO of the nitrone. These values are in agreement with the lower absolute value of the electronic chemical potential of vinyl acetate (μ=−0.12992) with respect to nitrones **2d**,**e** (μ=−0.13829 and −0.13449, respectively), with the exception of nitrones **2a**–**c**,**f**, whose μ values are lower. In these latter cases the difference between the electronic chemical potential of **2a**–**c**,**f** and **4** is too small to permit any deduction; conversely, the NPA charge transfer at TSs level is more reliable.

4. Conclusion

This study demonstrates that DFT calculations at the B3LYP/6-31G* level of theory can be used effectively and without a high computational cost for describing the cycloaddition reaction between *C*-hetaryl nitrones and both electron-poor and electron-rich dipolarophiles represented by methyl acrylate and vinyl acetate, respectively. As expected from the theory and previous studies, the performed calculations predict a greater asynchronicity of the cycloaddition with methyl acrylate with respect to the reaction with vinyl acetate. DFT calculations successfully reproduced experimental regio- and stereoselectivities although only from a qualitative point of view. The observed small differences are not enough to quantitatively predict the course of the reaction. Forthcoming studies with other relevant dipolar cycloaddition reaction models are currently under way.

Acknowledgements

We thank for their support our programs: the Spanish Ministry of Science and Technology (MCYT) and FEDER

Program (Project CTQ2004-0421) and the Government of Aragon; the Ministry of Instruction, University and Scientific Research (Rome, Italy) and Italian C.N.R. (Roma).

References and notes

1. (a) Martin, J. N.; Jones, R. C. F. *Synthetic Applications of 1,3-Dipolar Cycloaddition Chemistry towards Heterocycles and Natural Products*; Padwa, A., Pearson, W. H., Eds.; Wiley: Chichester, UK, 2002; pp 1–81; (b) Namboothiri, I. N. N.; Hassner, A. *Top. Curr. Chem.* **2002**, *216*, 1–49; (c) Demarch, P.; Figueredo, M.; Font, J. *Heterocycles* **1999**, *50*, 1213–1226; (d) Frederickson, M. *Tetrahedron* **1997**, *53*, 403–425; (e) DeShong, P.; Lander, S. W., Jr.; Leginus, J. M.; Dickson, C. M. *Advances in Cycloaddition*; Curran, D. P., Ed.; JAI: Greenwich, UK, 1988; Vol. 1, pp 87–128; (f) Confalone, P. N.; Huie, E. M. *Org. React.* **1988**, *36*, 1–173.
2. (a) Merino, P. *Science of Synthesis. Houben–Weyl Methods of Molecular Transformations*; Padwa, A., Ed.; Thieme: Stuttgart, 2004; Vol. 27, pp 511–580; (b) Ruck-Braun, K.; Freysoldt, T. H. E. *Chem. Soc. Rev.* **2005**, *34*, 507–516.
3. (a) Hüisgen, R.; Seidi, H.; Bruning, I. *Chem. Ber.* **1969**, *102*, 1102–1103; (b) Firestone, R. A. *Tetrahedron* **1977**, *33*, 3009–3039; (c) Huisgen, R. *Advances in Cycloaddition*; Curran, D. P., Ed.; JAI: Greenwich, UK, 1988; Vol. 1, pp 1–32; (d) Raimondi, L. *Gazz. Chim. Ital.* **1997**, *127*, 167–175; (e) Cardona, F.; Goti, A.; Brandi, A. *Eur. J. Org. Chem.* **2001**, 2999–3011; (f) Kanemasa, S. *Synlett* **2002**, 1371–1387; (g) Rastelli, A.; Gandolfi, R.; Amadè, M. S. *Adv. Quantum Chem.* **2000**, *36*, 151–167.
4. (a) Domingo, L. R.; Arnó, M.; Merino, P.; Tejero, T. *Eur. J. Org. Chem.* **2006**, 3464–3472; (b) Wanapun, D.; Van Gorp, K. A.; Mosey, N. J.; Kerr, M. A.; Woo, T. K. *Can. J. Chem.* **2005**, *83*, 1752–1767; (c) Kavitha, K.; Venuvanalingam, P. *Int. J. Quantum Chem.* **2005**, *104*, 64–78; (d) Sun, X. M.; Wang, M. H.; Liu, P.; Bian, W. S.; Feng, D. C.; Cai, Z. T. *J. Mol. Struct.: THEOCHEM* **2004**, *679*, 73–87; (e) Wagner, G. *Chem.—Eur. J.* **2003**, *9*, 1503–1510; (f) Rastelli, A.; Gandolfi, R.; Sarzi-Amadè, M.; Carboni, M. *J. Org. Chem.* **2001**, *66*, 2449–2458; (g) Domingo, L. R. *Eur. J. Org. Chem.* **2000**, 2265–2272; (h) Carda, M.; Portoles, R.; Murga, J.; Uriel, S.; Marco, J. A.; Domingo, L. R.; Zaragoza, R. J.; Roper, H. *J. Org. Chem.* **2000**, *65*, 7000–7009.
5. (a) Koumbis, A. E.; Gallos, J. K. *Curr. Org. Chem.* **2003**, *7*, 585–628; (b) Kaliappan, K. P.; Das, P.; Kumar, N. *Tetrahedron Lett.* **2005**, *46*, 3037–3040; (c) Shimizu, T.; Ishizaki, M.; Nitada, N. *Chem. Pharm. Bull.* **2002**, *50*, 908–921; (d) Cicchi, S.; Crea, S.; Goti, A.; Brandi, A. *Tetrahedron: Asymmetry* **1997**, *8*, 293–301; (e) Aurich, H. G.; Möbus, K. D. *Tetrahedron Lett.* **1988**, *29*, 5755–5758.
6. (a) Chiacchio, U.; Rescifina, A.; Romeo, G. *Targets in Heterocyclic Chemistry—Chemistry and Properties*; Attanasi, O. A., Spinelli, D., Eds.; Italian Society of Chemistry: Rome, Italy, 1997; Vol. 1, pp 225–276; (b) Merino, P. *Targets in Heterocyclic Chemistry—Chemistry and Properties*; Attanasi, O. A., Spinelli, D., Eds.; Italian Society of Chemistry: Rome, Italy, 2003; Vol. 7, pp 140–156; (c) Broggini, G.; Zecchi, G. *Synthesis* **1999**, 905–917; (d) Holmes, A. B.; Bourdin, B.; Collins, I.; Davison, E. C.; Rudge, A. J.; Stork, T. C.; Warner, J. A. *Pure Appl. Chem.* **1997**, *69*, 531–536.
7. (a) Romeo, G.; Iannazzo, D.; Piperno, A.; Romeo, R.; Corsaro, A.; Rescifina, A.; Chiacchio, U. *Mini-Rev. Org. Chem.* **2005**, *2*, 59–77; (b) Chiacchio, U.; Genovese, F.; Iannazzo, D.; Librando, V.; Merino, P.; Rescifina, A.; Romeo, R.; Procopio, A.; Romeo, G. *Tetrahedron* **2004**, *60*, 441–448; (c) Saita, M. G.; Chiacchio, U.; Iannazzo, D.; Corsaro, A.; Merino, P.; Piperno, A.; Previtera, T.; Rescifina, A.; Romeo, G.; Romeo, R. *Nucleosides, Nucleotides Nucleic Acids* **2003**, *22*, 739–742; (d) Merino, P.; Revuelta, J.; Tejero, T.; Chiacchio, U.; Rescifina, A.; Piperno, A.; Romeo, G. *Tetrahedron: Asymmetry* **2002**, *13*, 167–172.
8. (a) Merino, P.; Anoro, S.; Franco, S.; Merchán, F. L.; Tejero, T.; Tuñon, V. *J. Org. Chem.* **2000**, *65*, 1590–1596; (b) Tejero, T.; Dondoni, A.; Rojo, I.; Merchán, F. L.; Merino, P. *Tetrahedron* **1997**, *53*, 3301–3318; (c) Chiacchio, U.; Corsaro, A.; Mates, J. A.; Merino, P.; Piperno, A.; Rescifina, A.; Romeo, G.; Romeo, R.; Tejero, T. *Tetrahedron* **2003**, *59*, 4733–4738; (d) Broggini, G.; Chiesa, K.; De Marchi, I.; Martinelli, M.; Pilati, T.; Zecchi, G. *Tetrahedron* **2005**, *61*, 3525–3531; (e) Tamura, O.; Kanoh, A.; Yamashita, M.; Ishibayashi, H. *Tetrahedron* **2004**, *60*, 9997–10003; (f) Ishar, M. P. S.; Singh, G.; Kumar, K.; Singh, R. *Tetrahedron* **2000**, *56*, 7817–7828.
9. For reviews on the synthetic utility of heterocycles, see: (a) Lee, H. K.; Chan, K. F.; Hui, C. W.; Yim, H. K.; Wu, X. W.; Wong, H. N. C. *Pure Appl. Chem.* **2005**, *77*, 139–143; (b) Spanu, P.; Ulgheri, F.; Spinelli, D. *Targets in Heterocyclic Chemistry—Chemistry and Properties*; Attanasi, O. A., Ed.; Italian Society of Chemistry: Rome, Italy, 2004; Vol. 8, pp 330–342; (c) Dondoni, A.; Marra, A. *Chem. Rev.* **2004**, *104*, 2557–2599; (d) Wong, H. N. C.; Yu, P.; Yick, C. Y. *Pure Appl. Chem.* **1999**, *71*, 1041–1044; (e) Lipshutz, B. H. *Chem. Rev.* **1986**, *86*, 795–819.
10. Merino, P.; Anoro, S.; Merchán, F. L.; Tejero, T. *Molecules* **2000**, *5*, 132–152.
11. (a) Astolfi, P.; Bruni, P.; Greci, L.; Stipa, P.; Righi, L.; Rizzoli, C. *Eur. J. Org. Chem.* **2003**, 2626–2634; (b) See Ref. 8f; (c) Jedlovska, E.; Sapik, M.; Fišera, L. *Chem. Pap.* **1997**, *51*, 427–431; (d) Coutouli-Argyropoulou, E.; Malamidou-Xenikaki, E.; Stampelos, X. N.; Alexopoulou, I. N. *Tetrahedron* **1997**, *53*, 707–718; (e) Camiletti, C.; Poletti, L.; Trombini, C. *J. Org. Chem.* **1994**, *59*, 6843–6846.
12. Merino, P.; Revuelta, J.; Tejero, T.; Chiacchio, U.; Rescifina, A.; Romeo, G. *Tetrahedron* **2003**, *59*, 3581–3592.
13. The use of DFT methods has emerged as an excellent alternative to traditional ab initio methods, in particular, for the study of cycloaddition reactions. See: (a) Parr, R. G.; Yang, W. *Density Functional Theory of Atoms and Molecules*; Oxford University Press: New York, NY, 1989; (b) Ziegler, T. *Chem. Rev.* **1991**, *91*, 651–667; (c) Geerlings, P.; De Proft, F.; Langenaeker, W. *Chem. Rev.* **2003**, *103*, 1793–1873; (d) Herrera, R.; Nagarajan, A.; Morales, M. A.; Mendez, F.; Jimenez-Vazquez, H. A.; Zepeda, L. G.; Tamariz, J. *J. Org. Chem.* **2001**, *66*, 1252–1263; (e) Kuznetsov, M. L.; Kukushkin, V. Yu. *J. Org. Chem.* **2006**, *71*, 582–592.
14. Merino, P.; Anoro, S.; Merchán, F. L.; Tejero, T. *Heterocycles* **2000**, *53*, 861–876.
15. (a) Becke, A. D. *J. Chem. Phys.* **1993**, *98*, 5648–5652; (b) Becke, A. D. *Phys. Rev. A* **1988**, *38*, 3098–3100; (c) Lee, C.; Yang, W.; Parr, R. G. *Phys. Rev. B* **1988**, *37*, 785–789.
16. Reed, A. E.; Weinstock, R. B.; Weinhold, F. *J. Chem. Phys.* **1985**, *83*, 735–746.
17. Hehre, W. J.; Radom, L.; Schleyer, P.; von, R.; Pople, J. A. *Ab Initio Molecular Orbital Theory*; Wiley: New York, NY, 1986.
18. (a) Fukui, K. *Acc. Chem. Res.* **1981**, *14*, 363–368; (b) Head-Gordon, M.; Pople, J. A. *J. Chem. Phys.* **1988**, *89*, 5777–5786.

19. Frisch, M. J.; Trucks, G. W.; Schlegel, H. B.; Scuseria, G. E.; Robb, M. A.; Cheeseman, J. R.; Zakrzewski, V. G.; Montgomery, J. A., Jr.; Stratmann, R. E.; Burant, J. C.; Dapprich, S.; Millam, J. M.; Daniels, A. D.; Kudin, K. N.; Strain, M. C.; Farkas, O.; Tomasi, J.; Barone, V.; Cossi, M.; Cammi, R.; Mennucci, B.; Pomelli, C.; Adamo, C.; Clifford, S.; Ochterski, J.; Petersson, G. A.; Ayala, P. Y.; Cui, Q.; Morokuma, K.; Malick, D. K.; Rabuck, A. D.; Raghavachari, K.; Foresman, J. B.; Cioslowski, J.; Ortiz, J. V.; Stefanov, B. B.; Liu, G.; Liashenko, A.; Piskorz, P.; Komaromi, I.; Gomperts, R.; Martin, R. L.; Fox, D. J.; Keith, T.; Al-Laham, M. A.; Peng, C. Y.; Nanayakkara, A.; Gonzalez, C.; Challacombe, M.; Gill, P. M. W.; Johnson, B.; Chen, W.; Wong, M. W.; Andres, J. L.; Gonzalez, C.; Head-Gordon, M.; Replogle, E. S.; Pople, J. A. *Gaussian 03 Revision B.1*; Gaussian: Pittsburgh, PA, 2003.
20. Avalos, M.; Babiano, R.; Clemente, F. R.; Cintas, P.; Gordillo, R.; Jimenez, J. L.; Palacios, J. C. *J. Org. Chem.* **2000**, *65*, 8251–8259.
21. Aroney, M. J.; Bruce, E. A. W.; John, I. G.; Radom, L.; Ritchie, G. L. D. *Aust. J. Chem.* **1976**, *29*, 581–587.
22. *syn* and *anti* conformations refer to synperiplanar and antiperiplanar dispositions between the nitrone nitrogen and the heteroatom of the heterocyclic ring. In the case of the thiazole-derived nitrone **2d** nomenclature is referred to the sulfur atom.
23. (a) Breuer, E. Nitrones and Nitronic acid Derivatives: An Update. In *Nitrones, Nitronates and Nitroxides*; Patai, S., Rappoport, Z., Eds.; Wiley: Chichester, UK, 1989; pp 245–312; (b) Hamer, J.; Macaluso, A. *Chem. Rev.* **1964**, *64*, 473–495.
24. Merino, P.; Tejero, T.; Laguna, M.; Cerrada, E.; Moreno, A.; Lopez, J. A. *Org. Biomol. Chem.* **2003**, *1*, 2336–2342.
25. Reed, A. E.; Curtiss, L. A.; Weinhold, F. *Chem. Rev.* **1988**, *88*, 899–926.
26. (a) Minyaev, R. N.; Minkin, V. I. *Can. J. Chem.* **1998**, *76*, 776–788; (b) Hudson, R. F.; Wallis, J. D.; Hansell, D. P. *Heterocycles* **1994**, *37*, 1933–1950.
27. (a) Pearson, R. G. *J. Chem. Educ.* **1987**, *64*, 561–567; (b) Parr, R. G.; Chattaraj, P. K. *J. Am. Chem. Soc.* **1991**, *113*, 1854–1855.
28. Parr, R. G.; von Szentpály, L.; Liu, S. *J. Am. Chem. Soc.* **1999**, *121*, 1922–1924.
29. Domingo, L. R.; Aurell, M. J.; Perez, P.; Contreras, R. *Tetrahedron* **2002**, *58*, 4417–4423.
30. Perez, P.; Domingo, L. R.; Aurell, M. J.; Contreras, R. *Tetrahedron* **2003**, *59*, 3117–3125.
31. (a) Chandra, A. K.; Nguyen, M. T. *J. Phys. Chem. A* **1998**, *102*, 6181–6185; (b) Chandra, A. K.; Nguyen, M. T. *J. Comput. Chem.* **1998**, *19*, 195–202; (c) Nguyen, T. L.; De Proft, F.; Chandra, A. K.; Uchimaru, T.; Nguyen, M. T.; Geerlings, P. *J. Org. Chem.* **2001**, *66*, 6096–6103; (d) Sengupta, D.; Chandra, A. K.; Nguyen, M. T. *J. Org. Chem.* **1997**, *62*, 6404–6406; (e) Damoun, S.; Van de Woude, G.; Mendez, F.; Geerlings, P. *J. Phys. Chem. A* **1997**, *101*, 886–893.
32. (a) Parr, R. G.; Pearson, R. G. *J. Am. Chem. Soc.* **1983**, *105*, 7512–7516; (b) See Ref. 13a.
33. Mayo, P.; Hecnar, T.; Tam, W. *Tetrahedron* **2001**, *57*, 5931–5941.
34. (a) Loncharich, R. J.; Brown, F. K.; Houk, K. N. *J. Org. Chem.* **1989**, *54*, 1129–1134; (b) Birney, D. M.; Houk, K. N. *J. Am. Chem. Soc.* **1990**, *112*, 4127–4133; (c) Apeloig, Y.; Matzer, E. *J. Am. Chem. Soc.* **1995**, *117*, 5375–5376.
35. Aurell, M. J.; Domingo, L. R.; Perez, P.; Contreras, R. *Tetrahedron* **2004**, *60*, 11503–11509.
36. Wiberg, K. B. *Tetrahedron* **1968**, *24*, 1083–1096.
37. (a) Carpenter, J. E.; Weinhold, F. *J. Mol. Struct.: THEOCHEM* **1988**, *169*, 41–62; (b) See Ref. 16.
38. (a) Merino, P.; Anoro, S.; Cerrada, E.; Laguna, M.; Moreno, A.; Tejero, T. *Molecules* **2001**, *6*, 208–220; (b) See Ref. 10.